

# Επιστημονικό Συνέδριο προς τιμήν του ομοτ. καθηγητή ΕΜΠ Γεράσιμου Αθανασούλη

4-5 Ιουλίου 2022, ΕΜΠ, Αθήνα

# Shape-optimization of 2D hydrofoils using one-way coupling of an IGA-BEM solver with the boundary-layer model

C.G. Politis<sup>1</sup>, K.V. Kostas<sup>2</sup>, A.I. Ginnis<sup>3</sup>, P.D. Kaklis<sup>4</sup>

4-5 July 2022, Athens

---

<sup>1</sup>University of West Attica, Greece

<sup>2</sup>Nazarbayev University, KZ

<sup>3</sup>National Technical University of Athens, Greece

<sup>4</sup>University of Strathclyde UK

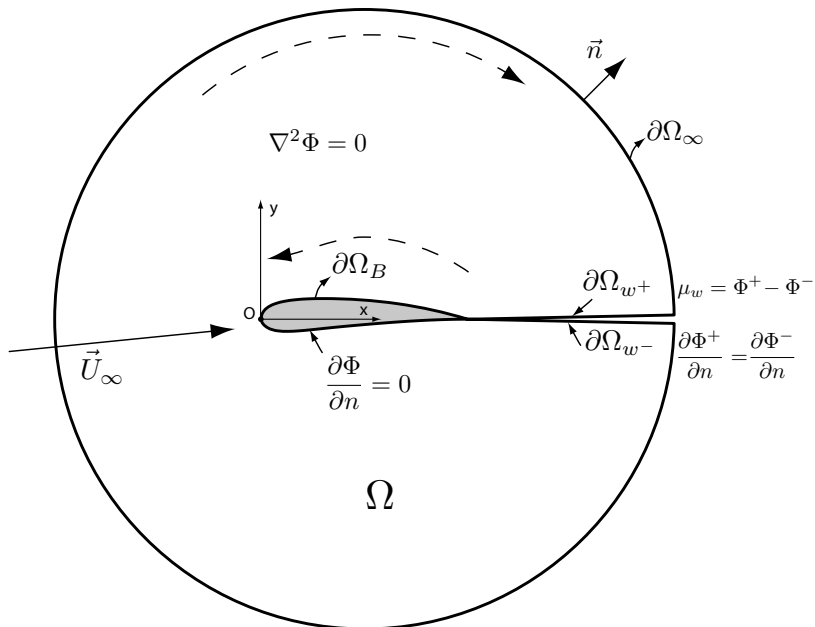
# Contents

- 1 Formulation of the problem
- 2 A discrete IGA-BEM formulation
- 3 Numerical Results
- 4 Boundary-layer corrections
- 5 Shape optimization

# Formulation of the problem

We consider a two-dimensional body whose boundary is  $\partial\Omega_B$ , moving with constant speed  $\vec{U}_B$  in an ideal fluid of infinite extent.

In a body-fixed coordinate system  $Oxy$  this problem is equivalent to a uniform stream with velocity  $\nabla\Phi_\infty = \vec{U}_\infty = -\vec{U}_B$ , where  $\Phi_\infty(\mathbf{P}) = u_\infty x + v_\infty y$  is the far-field asymptotic form of the velocity potential  $\Phi(\mathbf{P})$  of the resulting flow at point  $\mathbf{P}=(x, y)$ .



# Differential formulation

The potential  $\Phi(\mathbf{P})$  is the solution of the following boundary-value problem (BVP):

$$\nabla^2 \Phi = 0, \quad \mathbf{P} = (x, y) \in \Omega, \quad (1)$$

$$\frac{\partial \Phi}{\partial n} = 0, \quad \mathbf{P} \in \partial\Omega_B, \quad (2)$$

$$\Phi - (u_\infty x + v_\infty y) \rightarrow 0, \quad \text{as } x^2 + y^2 \rightarrow \infty, \quad (3)$$

where  $\Omega$  is the fluid domain outside  $\partial\Omega_B$  and  $\vec{n}$  denotes the unit normal vector on  $\partial\Omega_B$  directed inwards with respect to the body.

# Wake

The above BVP has a unique solution up to an additive constant and, in order to fix a unique solution, we normally consider, for smooth bodies, zero circulation  $\Gamma(C) = \int_C \nabla\Phi \cdot d\mathbf{c}$  of the velocity field  $\nabla\Phi$  over any circuit  $C$  surrounding the body.

The difference between potential flows around a smooth body and a hydrofoil is that, in order for the flow around the hydrofoil to have a physical meaning, the circulation has to be nonzero and appropriately adjusted until the flow leaves the trailing edge smoothly.

More specifically, on the basis of Kelvin's theorem, Prandtl concluded that if an airfoil, which started its motion from rest in an ideal fluid, is later found to possess non-zero circulation  $\Gamma$ , then the component of the boundary of the fluid which coincided with the airfoil initially, must coincide at a later time with the union of the airfoil surface and a surface, the so-called *wake*, embedded in the fluid which has circulation  $-\Gamma$ .

# Wake

In contrast to the 3D case, the location and shape of the wake in the 2D case can be taken, without loss of generality, to be a straight line emanating from the trailing edge and extending to infinity. This line is a force-free boundary along which the normal fluid velocity and the pressure should exhibit no jump. More accurately, we can write:

$$\frac{\partial \Phi^+}{\partial n} = \frac{\partial \Phi^-}{\partial n}, \quad \mathbf{P} \in \partial\Omega_w : \text{kinematic boundary condition}, \quad (4)$$

$$p^+ = p^-, \quad \mathbf{P} \in \partial\Omega_w : \text{dynamic boundary condition} \quad (5)$$

where,  $\Phi^\pm / p^\pm$  denote the velocity potential / pressure on the upper,  $\partial\Omega_{w+}$ , and lower,  $\partial\Omega_{w-}$ , face of the wake boundary, respectively.



# Boundary Integral Equation Formulation

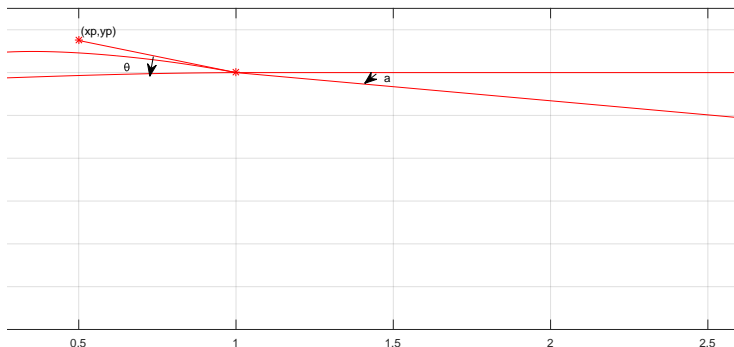
Applying in  $\Omega$  Green's second identity between the potential  $\Phi(\mathbf{P})$ ,  $\mathbf{P} \in \Omega$ , and the fundamental solution,  $G(\mathbf{P}, \mathbf{Q}) = (1/2\pi) \ln \|\mathbf{P} - \mathbf{Q}\|$ , of the 2D Laplace equation, we can reformulate the BVP as a 2<sup>nd</sup>-kind Fredholm integral equation on the hydrofoil boundary  $\partial\Omega_B$ , taking into account the wake-sheet kinematic boundary condition:

$$\frac{\Phi(\mathbf{P})}{2} - \int_{\partial\Omega_B} \Phi(\mathbf{Q}) \frac{\partial G(\mathbf{P}, \mathbf{Q})}{\partial n_Q} ds_Q - \mu_w \int_{\partial\Omega_w} \frac{\partial G(\mathbf{P}, \mathbf{Q})}{\partial n_Q} ds_Q = \Phi_\infty(\mathbf{P}),$$

$$\mathbf{P} \in \partial\Omega_B \setminus \mathbf{P}_{TE}, \quad (6)$$

where  $\mu_w$  denotes the circulation around the hydrofoil and  $\mathbf{P}_{TE} = (x_e, y_e)$  its trailing edge.

# Elaboration of wake-term



$$\int_{\partial\Omega_w} \frac{\partial G(\mathbf{P}, \mathbf{Q})}{\partial n_Q} ds_Q = \frac{1}{2\pi} (a - \theta) \quad (7)$$

revealing that the influence of the wake to the fluid flow is equivalent to a point vortex located at the trailing edge.

# Kutta conditions

In order to solve the lifting problem we have to specify the Kutta condition at the trailing edge.

- **Kinematic Kutta Condition:** The equation

$$\mu_w = \Phi^+(\mathbf{P}_{TE}) - \Phi^-(\mathbf{P}_{TE}). \quad (8)$$

is the so-called *Morino-Kutta condition*, stating that the proper value of circulation  $\Gamma$  around the hydrofoil equals to the potential jump at the trailing edge.

# Kutta conditions

- Dynamic Kutta Condition:** The zero pressure jump at the trailing edge ( $p_{TE}^+ = p_{TE}^-$ ) is another form of the Kutta condition (see eq. 5). This is equivalent to the statement that the total velocities on the upper and lower faces of the trailing edge should be equal.

$$\left( \frac{\partial \Phi^+(\mathbf{P}_{TE})}{\partial s} \right) = \left( \frac{\partial \Phi^-(\mathbf{P}_{TE})}{\partial s} \right) \quad (9)$$

We recall here that in the case of a hydrofoil with finite trailing-edge angle the velocities at the trailing edge should be zero. However, this requirement seems to be very stiff, from the numerical point of view, and may be relaxed to the condition of equal velocity amplitudes on the upper and lower faces of the trailing edge, which may be finite.

# Kutta conditions

- **Mixed Kutta Condition:** It is a combination of the kinematic and dynamic Kutta conditions.

$$\mu_w = \Phi^+(\mathbf{P}_{TE}) - \Phi^-(\mathbf{P}_{TE}). \quad (10)$$

$$p_{TE}^+ = p_{TE}^- \quad (11)$$

In this case the resulting linear system has to be solved in the least square sense.

# The IGA basis

We assume that the body boundary  $\partial\Omega_B$  can be (accurately) represented as a closed parametric NURBS curve  $\mathbf{r}(t)$ ,  $t \in [0, 1]$ , which is regular, i.e., the derivative vector is well defined and not vanishing, with the exception of the trailing edge:  $\mathbf{r}(0) = \mathbf{r}(1)$ , where the derivative vector is not defined. More specifically,

$$\mathbf{r}(t) = (x(t), y(t)) := \sum_{i=0}^n \mathbf{d}_i M_{i,k}(t), \quad t \in I = [t_{k-1}, t_{n+1}] := [0, 1], \quad (12)$$

where  $\{M_{i,k}(t)\}_{i=0}^n$  is a rational  $B$ -spline basis of order  $k$ , defined over a knot sequence  $\mathcal{J} = \{t_0, t_1, \dots, t_{n+k}\}$  and possessing non-negative weights  $w_i$ ,  $i = 0, \dots, n$ , while  $\mathbf{d}_i$  are the associated control points.

# The Boundary-Integral Equation

The Boundary-Integral Equation is written in the following form:

$$\frac{\phi(t)}{2} - \int_I \phi(\tau) K(t, \tau) d\tau - \frac{\mu_w}{2\pi} \arctan \left( \frac{y(t) - y_e}{x(t) - x_e} \right) = g(t), \quad t \in (0, 1), \quad (13)$$

where, for the sake of simplicity, we define

$$\phi(t) := \phi(\mathbf{r}(t))$$

$$G(t, \tau) := G(\mathbf{r}(t), \mathbf{r}(\tau)) \text{ and}$$

$$K(t, \tau) = (\partial G(t, \tau) / \partial n_\tau) \|\dot{\mathbf{r}}(\tau)\|$$

# A spline space for the perturbation potential $\phi(t)$

We project, in a suitably defined manner, the perturbation potential  $\phi(t)$  on the spline space  $\mathcal{S}^k(\mathcal{J}^{(\ell)})$ ,  $\mathcal{S}^k(\mathcal{J}^{(0)}) := \mathcal{S}^k(\mathcal{J})$ , expressed in the form:

$$\phi_s(t) := \mathcal{P}_s(\phi(t)) = \sum_{i=0}^{n+\ell} \phi_i M_{i,k}^{(\ell)}(t), \quad t \in I, M_{i,k}^{(0)}(t) := M_{i,k}(t), \quad (14)$$

where  $\ell \in \mathbb{N}_0$  denotes the number of knots inserted in  $I$ .

Recalling the fundamental property of knot insertion, we can say that  $\{\mathcal{S}^k(\mathcal{J}^{(\ell)}), \ell \in \mathbb{N}_0\}$  constitutes a sequence of nested finite dimensional-spaces, i.e.,  $\mathcal{S}^k(\mathcal{J}^{(\ell)}) \subset \mathcal{S}^k(\mathcal{J}^{(\ell+1)})$ .



# Discretization of the BIE

The projection of  $\phi(t)$  on  $\mathcal{S}^k(\mathcal{J}^{(\ell)})$  is materialized through interpolation at a set of collocation points  $t = t_j$ ,  $j = 0, \dots, n + \ell$ , which are chosen to be the Greville abscissas. This leads to the following linear system for the unknown coefficients  $\phi_i$ ,  $i = 0, \dots, n + \ell$ :

$$\frac{1}{2} \sum_{i=0}^{n+\ell} \phi_i M_{i,k}^{(\ell)}(t_j) - \sum_{i=0}^{n+\ell} \phi_i q_i(t_j) - \frac{\mu_w}{2\pi} \arctan \left( \frac{y(t_j) - y_e}{x(t_j) - x_e} \right) = g(t_j),$$

$$j = 0, \dots, n + \ell, \quad (15)$$

where  $q_i(t_j) = \int_I M_{i,k}^{(\ell)}(\tau) K(t_j, \tau) d\tau$ .

Since  $t \in (0, 1)$ , one must consider shifting the values of the first and the last Greville abscissa by a small value  $\epsilon > 0$ .

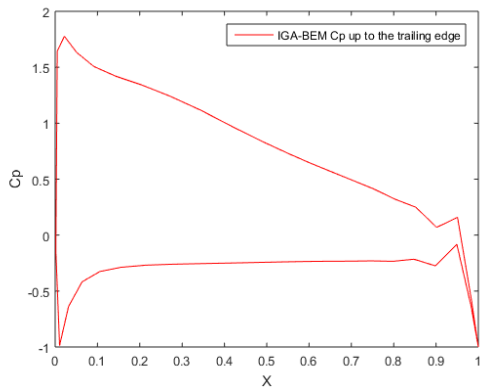


Figure:  $C_p$  along the hydrofoil. Fluid velocities at the trailing edge are enforced to be zero.

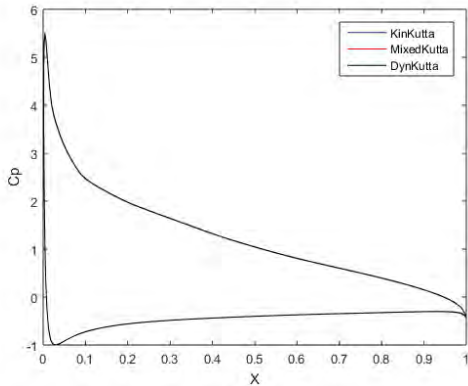


Figure:  $C_p$  along the hydrofoil, using different Kutta conditions.

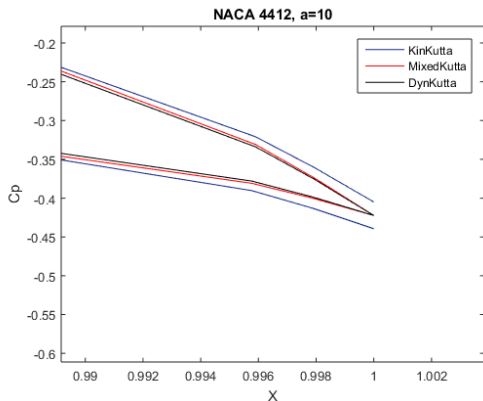
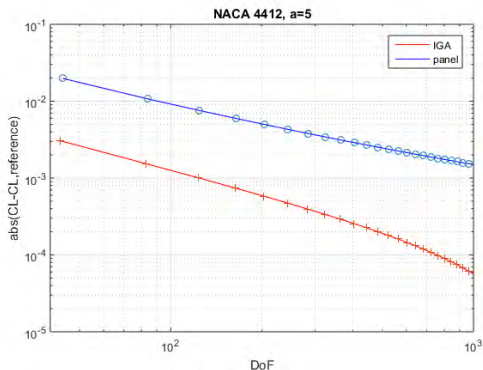


Figure:  $C_p$  along the hydrofoil, using different Kutta conditions. Zoom at the trailing edge.

# Error rate of convergence



**Figure:** Error of  $C_L$  of a NACA 4412 hydrofoil wrt DoF. Reference solution is calculated by IGA-BEM with a large number of DoFs ( $\approx 5000$ ).

# Boundary-layer (BL) model

- For an incompressible turbulent flow past an airfoil viscous effects are important in a small region around the foil
- In this region N-S (Navier-Stokes) equations are approximated by the so-called BL equations
- The BL model composes:
  - ① A model for the laminar part of the flow
  - ② A criterion for the transition point between the laminar and the turbulent flow
  - ③ A model for the turbulent part of the flow

# A one-way coupled computation model

We adopt a simple one-way coupled computation model consisting of:

- Thwaites' one equation for laminar flow
- Head's two equations for turbulent flow
- Michel's criterion for the transition point
- Squire-Young formula for the drag coefficient

## Laminar model: Thwaites' one equation

## Von-Karman integral momentum equation

$$\frac{d\theta}{dx} + (2 + H)\frac{\theta}{U_e} \cdot \frac{dU_e}{dx} = \frac{1}{2}C_f \quad (16)$$

- $x/y$  are curvilinear coordinates measured tangentially/normal to the airfoil boundary from the stagnation point
- $U_e(x)$  is the free-stream velocity outside the boundary layer

$$\theta = \int_0^\infty \frac{u}{U_e} \cdot \left(1 - \frac{u}{U_e}\right) dy \quad : \quad \text{momentum thickness} \quad (17)$$

$$H = \frac{\delta^*}{\theta} \quad : \quad \text{shape factor, } \delta^* = \int_0^\infty \left(1 - \frac{u}{U_e}\right) dy \quad : \quad \text{displacement thickness}$$

$$C_f = \frac{\mu \frac{\partial u}{\partial y} \big|_{y=0}}{\frac{1}{2}\rho U_e^2} \quad : \quad \text{skin - friction coefficient} \quad (18)$$



# Laminar Model: Thwaites' assumption

After some manipulation on (16) we get:

$$\frac{U_e}{\nu} \cdot \frac{d\theta^2}{dx} = 2[(2 + H)m + I(m)] := L(m) \quad (19)$$

where,

$$m = \left( \frac{\theta^2}{U_e} \right) \frac{\partial^2 u}{\partial y^2} \Big|_{y=0}, \quad I(m) = \frac{\theta}{U_e} \cdot \frac{\partial u}{\partial y} \Big|_{y=0}$$

**Thwaites' assumption** There should be a function relating  $m$  and  $I(m)$ . He suggested the form  $L(m) = 0.45 + 6m$ , which reduces Von-Karman equation to an ODE with respect  $\theta(x)$ .

# Laminar Model: Thwaites' ODE

## Thwaites' ODE

$$U_e \frac{d}{dx} \left( \frac{\theta^2}{\nu} \right) = 0.45 - 6 \left( \frac{\theta^2}{\nu} \right) \frac{\partial U_e}{\partial x}$$

which is integrated to

$$\theta^2(x) = \left[ \frac{U_e(0)}{U_e(x)} \right]^6 \theta^2(0) + \frac{0.45\nu}{U_e^6(x)} \int_0^x U_e^5(x') dx'$$

with,

$$\theta(0) = \left( \frac{0.75\nu}{dU_e/dx|_{x=0}} \right)^{1/2}$$

- Separation of laminar flow cannot be predicted

# Michel's criterion for transition point

Transition should be expected when:

$$Re_{\theta} > Re_{\theta_{max}} = 1.174 \left( 1 + \frac{22.4}{Re_x} \right) Re_x^{0.46}$$

where,

$$Re_{\theta} = \frac{U_e \theta}{\nu}, \quad Re_x = \frac{U_e x}{\nu}$$

# Turbulent model: Head's equations

- Starting from Von-Karman integral momentum equation and introducing the parameter  $H_1 = (\delta - \delta^*)/\theta$ , where  $\delta$  is the thickness of the boundary layer, we obtain Head's system of equations:

$$\frac{d\theta}{dx} + (2 + H) \frac{\theta}{U_e} \cdot \frac{dU_e}{dx} = \frac{1}{2} C_f$$

$$\frac{dH_1}{dx} = -H_1 \left( \frac{1}{U_e} \cdot \frac{dU_e}{dx} + \frac{1}{\theta} \cdot \frac{d\theta}{dx} \right) + \frac{0.0306}{\theta} (H_1 - 3)^{-0.619}$$

- Semi-empirical relations are used to close the system

$$H_1 = \begin{cases} 3.3 + 0.8234(H - 1.1)^{-1.287}, & H \leq 1.6, \\ 3.3 + 1.5501(H - 0.6778)^{-3.064}, & H > 1.6. \end{cases}$$

# Turbulent model

- For the numerical solution of Head's equations a 2nd-order Runge-Kutta scheme is used.
- Turbulent separation can be predicted. The separation criterion is given by:  $H_1 = 3.3$

# The Drag coefficient

## Squire-Young formula for the drag coefficient

$$C_d = \left[ 2\theta_{TE}(U_e) \frac{H_{TE}^{+5}}{2} \right]_{UP} + \left[ 2\theta_{TE}(U_e) \frac{H_{TE}^{+5}}{2} \right]_{LOW}$$

The above formula predicts the drag coefficient by relating the momentum defect far downstream to the values of the flow field at both sides of the trailing edge (TE).

# IGA-oriented BL corrections

## PABLO software

- PABLO stands for *"Potential flow around Airfoils with Boundary Layer coupled One-way"*
- It is a subsonic airfoil analysis program developed in MATLAB by C. Wauquier and A. Rizzi.

## IGA enhancements of PABLO

- We replace PABLO's low order panel approximation of the free-stream velocity  $U_e$  outside the boundary layer by its NURBS representation obtained using the derivative of the IGA-BEM rational B-spline basis.
- We replace the numerical approximation of  $\frac{dU_e}{dx}$  by its exact value using the NURBS representation of  $U_e$ .

# The shape-optimization environment

## The components of the optimization environment

- The optimization Algorithm
- THE IGA-BEM solver
  - inviscid fluid
  - inviscid fluid with BL corrections
- The Geometric Parametric Modeler



# The Geometric Parametric Modeler

- The parametric model for a general hydrofoil has been materialized within Rhinoceros 3D modeling software package with the aid of its VBscript-based programming language, Rhinoscript.
- The model generates a closed cubic B-Spline curve that represents a hydrofoil, using a set of 11 parameters.

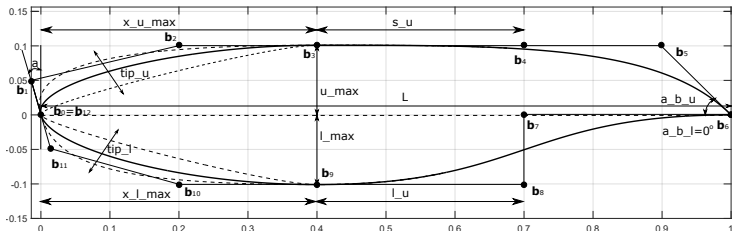


**Figure:** Foil instance corresponding to design vector  $\mathbf{v} = (v_i)$ ,  $v_i = 0.5, i = 1, \dots, 10, v_{11} = 0.1$

# The Geometric Parametric Modeler

- all parameters, with the exception of chord's length ( $L$ ), are defined using appropriate non-dimensional ratios so that their values always lie in  $[0; 1]$
- This approach eliminates the need of implementing complex interdependent constraints while guaranteeing the robustness of the procedure which is of significant importance in an optimization procedure

# The Geometric Parametric Modeler

Table: Parameters' definition

Nr.	Name	description	symbol	actual range
0	Length	Length of foil's chord	L	free
1	Upper-side max width	Maximum width of suction side w.r.t. chord	u_max	$[0, 1] \rightarrow \left[ \frac{L}{500}, \frac{L}{5} \right]$
2	Upper-side max width position	Longitudinal position of suction side's max width	x_u_max	$[0, 1] \rightarrow \left[ \frac{L}{10}, \frac{7L}{10} \right]$
3	Upper-side angle	Suction's side angle at trailing edge w.r.t. chord	a_b_u	$[0, 1] \rightarrow [0, 90]^\circ$
4	Upper-side tip shape	Leading edge upper part form factor	tip_u	$[0, 1] \rightarrow [0.1, 0.9]$
5	Upper-side aft-part shape	Inflection point position and/or shape fullness	s_u	$[0, 1] \rightarrow [0.05, 0.95](L - x_u\_max)$
6	Lower-side max width	Maximum width of lower side w.r.t. chord	l_max	$[0, 1] \rightarrow \left[ \frac{L}{500}, \frac{L}{5} \right]$

Table: Parameters' definition

Nr.	Name	description	symbol	actual range
7	Lower-side max width position	Longitudinal position of lower side's max width	$x_{l\_max}$	$[0, 1] \rightarrow \left[ \frac{L}{10}, \frac{7L}{10} \right]$
8	Lower-side angle	Suction's side angle at trailing edge w.r.t. chord	$a_{b\_l}$	$[0, 1] \rightarrow [-a_{b\_l}, a_{b\_l}]^\circ$
9	Lower-side tip shape	Leading edge upper part form factor	$tip\_l$	$[0, 1] \rightarrow [0.1, 0.9]$
10	Lower-side aft-part shape	Inflection point position and/or shape fullness	$s\_l$	$[0, 1] \rightarrow [0.05, 0.95](L - x_{l\_max})$
11	Tangent angle at leading edge	The angle between the vertical axis and foil's tangent direction at the leading edge	$a$	$[0, 1] \rightarrow [-20, 20]^\circ$

# The optimization Algorithm

- The selected optimization algorithm belongs to the category of evolutionary ones, as experimentation with gradient and hessian-based algorithms has indicated the existence of multiple local minima that makes their usage problematic
- Our optimizer uses the multi-objective optimization method gamultiobj which employs a controlled elitist genetic algorithm (GA)
- An elitist GA always favors individuals with better fitness value (rank)
- A controlled elitist GA also favors individuals that can help increase the diversity of the population even if they have a lower fitness value
- It is important to maintain the diversity of population for convergence to an optimal Pareto front

# An optimization example

## Optimization criteria

- Inviscid model: maximize lift coefficient  $C_L$
- BL model: minimize  $C_d/C_L$
- Minimum deviation from a reference area

## Optimization assumptions

- The reference area is set to be the one of the NACA-4412 profile
- The IGA-BEM solver produces an average lift coefficient calculated for three angles of attack, namely 1, 3 and 5 degrees
- The parameter Length (L) of the hydrofoil parametric model is assumed to be fixed and is regularized to one

# Shape-optimization results: Inviscid model

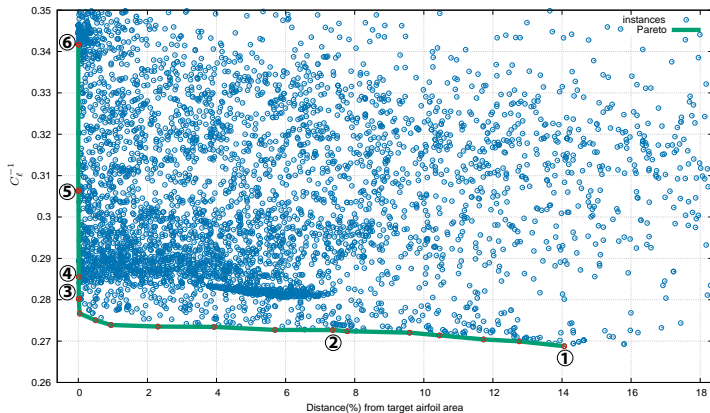


Figure: Pareto front for the inverse of the average lift coefficient and the area-deviation criteria.

## Shape-optimization results: Inviscid model

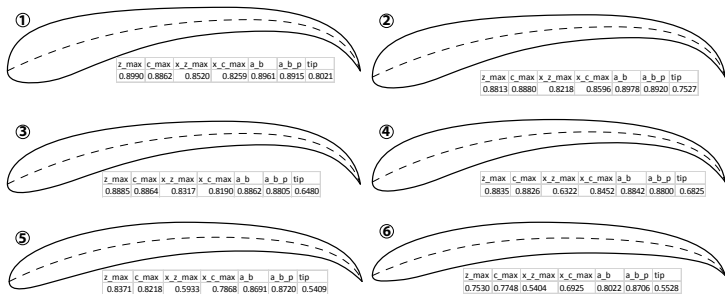


Figure: Instances of the hydrofoils depicted on the Pareto front. Decreasing lift coefficient in a left-to-right, top-to-bottom fashion.



# Shape-optimization results: BL-corrections

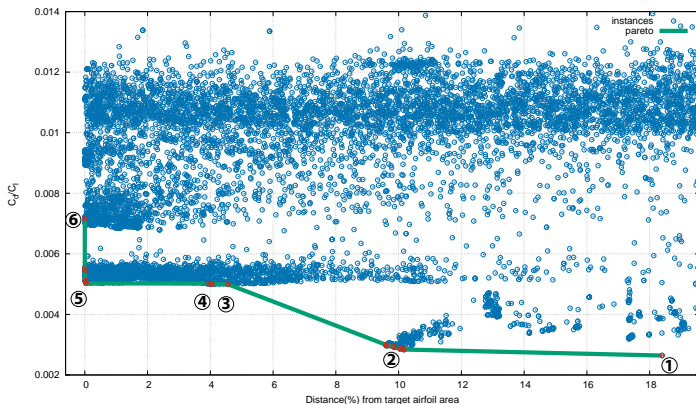


Figure: Pareto front for the drag to lift coefficient ratio and the area-deviation criteria.

# Shape-optimization results: BL-corrections

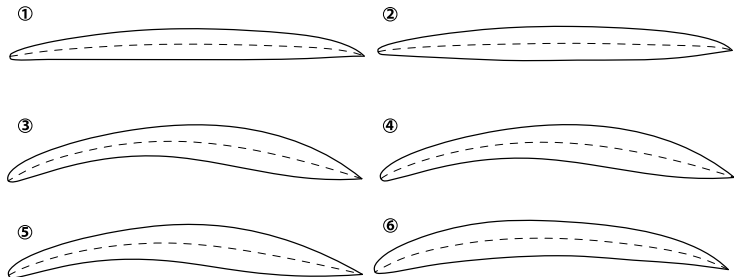


Figure: Instances of the hydrofoils depicted on the Pareto front.